ISSN 1063-7761, Journal of Experimental and Theoretical Physics, 2014, Vol. 118, No. 1, pp. 104–110. © Pleiades Publishing, Inc., 2014.
Original Russian Text © D.A. Balaev, D.M. Gokhfeld, S.I. Popkov, K.A. Shaikhutdinov, L.A. Klinkova, L.N. Zherikhina, A.M. Tsvokhrebov, 2014, published in Zhurnal Eksperimental'noi i Teoreticheskoi Fiziki, 2014, Vol. 145, No. 1, pp. 120–127.

ORDER, DISORDER, AND PHASE TRANSITION IN CONDENSED SYSTEM

Increase in the Magnetization Loop Width in the $Ba_{0.6}K_{0.4}BiO_3$ Superconductor: Possible Manifestation of Phase Separation

D. A. Balaev[a], D. M. Gokhfeld[a], S. I. Popkov[a], K. A. Shaikhutdinov[a], L. A. Klinkova[b], L. N. Zherikhina[c], and A. M. Tsvokhrebov[c]

[a] *Kirensky Institute of Physics, Siberian Branch, Russian Academy of Sciences, Krasnoyarsk, 660036 Russia*
[b] *Institute of Solid State Physics, Russian Academy of Sciences, Chernogolovka, Moscow oblast, 142432 Russia*
[c] *Lebedev Physical Institute, Russian Academy of Sciences, Moscow, 119991 Russia*
e-mail: gokhfeld@iph.krasn.ru

Received May 16, 2013

Abstract—The magnetization of $Ba_{0.6}K_{0.4}BiO_3$ samples in fields up to 90 kOe in the temperature range from 2 to 30 K is investigated. It is shown that the observed increase in the width of the magnetization loop can be explained by a decrease in the phase nonuniformity upon an increase in the magnetic field. The asymmetric hysteretic dependence of magnetization with the secondary peak was successfully described by the extended critical state model taking into account the phase separation in the superconductor.

DOI: 10.1134/S1063776114010038

1. INTRODUCTION

An increase in the width of the magnetization loop (peak effect, fishtail) is manifested as a secondary peak of the hysteretic magnetization loop $M(H)$ and is often observed in various superconducting materials [1]. The peak effect is usually associated with the increase in the critical current with the field. Such an atypical field dependence of the critical current can be due to enhancement of vortex pinning associated with a change in the structure of the magnetic vortex lattice [2, 3] in strongly anisotropic superconductors [4]. The peak effect can also occur as a result of an increase in the number of pinning centers due to the formation of nuclei of the nonsuperconducting phase in the material [5–7].

The $Ba_xK_{1-x}BiO_3$ cubic superconductor (referred henceforth as BKBO) with a superconducting transition temperature of $T_c \approx 30$ K exhibits weak anisotropy of magnetic properties [8]; nevertheless, its magnetization loops demonstrate the peak effect. BKBO possesses a number of properties typical of high-temperature superconductors [9], such as broadening of the resistive transition in a magnetic field [10] and the presence of the vortex glass phase [11]. However, BKBO also demonstrates anomalous features in the magnetic and transport characteristics. According to the results obtained in [12, 13], polycrystalline BKBO samples as well as its single crystals have nonmonotonic dependences of resistance R on external field H, temperature T, and transport current; the retrieval of the resistive state from the superconducting state is also observed upon a decrease in temperature. In addition, S-shaped current—voltage (I–V) characteristics with a wide hysteresis loop were observed for BKBO crystals. Such effects were also observed in part in analysis of the transport properties (I–V curves, $R(H)$, and $R(T)$) for the $Sr_{1-x}K_xBiO_3$ and $Ba_{1-x}K_xBiO_3$ systems (with various values of x) [14–16] and allied compound $Ba_{0.25}Pb_{0.75}BiO_3$ ($T_c \sim 12$ K) [17–19]. These peculiarities can be interpreted on the basis of the model of a spatially inhomogeneous superconductor–insulator state [20] as applied to the given systems. Such an approach to describing the anomalous transport properties of BKBO was proposed for the first time in [12]. According to [20], if the Fermi level in a strongly degenerate semiconductor lies near the edge of the band gap, phase separation into the insulating and superconducting zones may take place in a chemically homogeneous material after the occurrence of superconductivity. The $Ba_{1-x}K_xBiO_3$ system is a semiconductor only when $x < 0.37$ [21]. At the same time, BKBO is a poor metal for $x > 0.37$, and its electron structure is close to that of a strongly degenerate semiconductor; the density of states at the Fermi surface is low [22] in spite of a fairly high T_c. A model of phase separation into the Fermi- and Bose-subsystems for BKBO, which describes the metal–insulator transitions for $x = 0.37$, was proposed in [23].

A system with spatial phase nonuniformities [20, 23] responds to an external magnetic field because phase separation must change during the suppression of the superconducting gap, tuning itself to new conditions self-consistently [13]. It remains unclear whether phase separation can be manifested in the magnetization curves of a superconductor.

In this study, we investigate the magnetization loops of a $Ba_{0.6}K_{0.4}BiO_3$ single crystal. The extended model of the critical state [24, 25], which was devel-

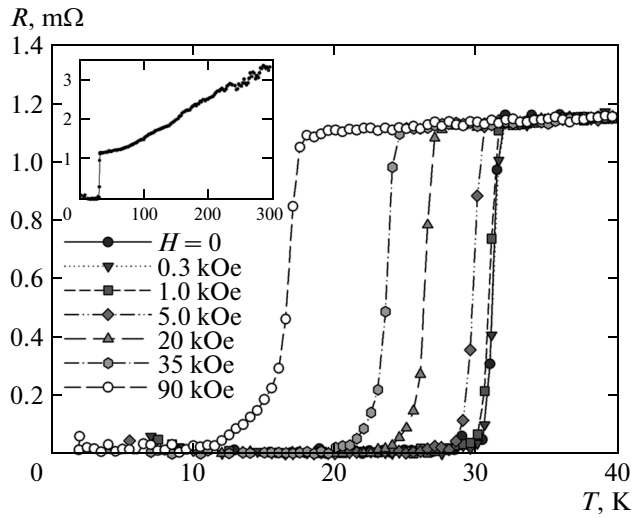

Fig. 1. Resistive transition in $Ba_{0.6}K_{0.4}BiO_3$ in various magnetic fields (transport current $I = 1$ mA). The inset shows the $R(T)$ dependence up to $T = 300$ K in zero external field.

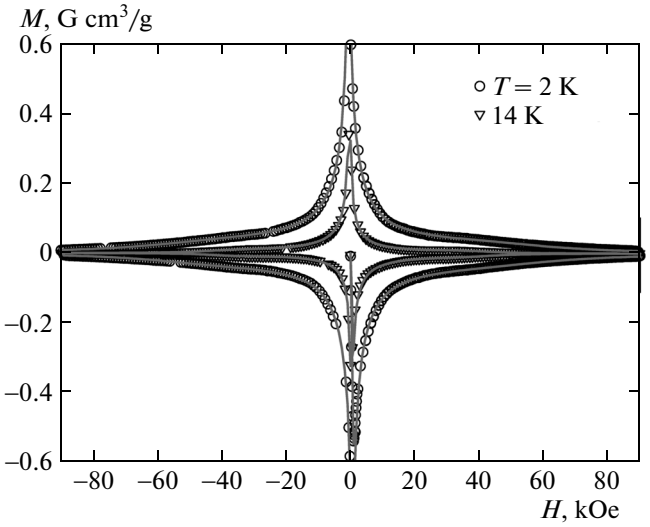

Fig. 2. Magnetization loops for $Ba_{0.6}K_{0.4}BiO_3$ at $T = 2.14$ K. Symbols correspond to experiment; curves are calculated using ECSM with allowance for phase separation (4).

oped to take into account the asymmetry and the secondary peak on the magnetization loop, is used for describing and determining the parameters of experimental $M(H)$ dependences. Possible reasons for the occurrence of the secondary peak in the field dependence of the magnetizations are analyzed. It is shown that the inclusion of phase separation into the extended model of the critical state makes it possible to describe all observed singularities on magnetization loops.

2. EXPERIMENT

Single-crystal samples $Ba_{0.6}K_{0.4}BiO_3$ were grown using the technique of chemical transport reactions [26]. The temperature dependences of resistance were measured by the standard four-probe method. The sample size was $1 \times 1 \times 0.8$ mm and the measuring current was 1 mA. The external field was applied at right angles to the transport current.

The magnetic properties were investigated using a PPMS-6000 vibrational magnetometer (Quantum Design). The sample mass was 59.6 mg. The magnetization data were corrected taking into account the diamagnetic signal of the sample holder insert. The magnetization hysteretic loops $M(H)$ were measured during sample cooling in the field of the Earth.

Figure 1 shows the temperature dependences of the resistance in various applied magnetic fields. The temperature corresponding to the beginning of the resistive transition T_c was approximately 31.8 K. At the same temperature, a diamagnetic signal appears on the temperature dependence of the magnetic moment in weak (a few oersteds) external magnetic fields. The temperature dependence of the upper critical field $H_{c2}(T)$ was determined from the $R(T)$ dependences measured in different magnetic fields: the temperature at which the extrapolations of the region with the normal resistance and the region of the sharp decrease in the resistance due to the superconducting transition intersect was fixed for each $R(T)$ dependence. The temperature T_{c0} at which dissipation appeared was determined from the $R(T)$ dependence from the criterion 5×10^{-6} Ω.

Figures 2–4 demonstrate typical features of the magnetization loops at various temperatures. At low temperatures, the $M(H)$ dependences are symmetric about the abscissa axis (Fig. 2). The secondary peak on the $M(H)$ dependences is manifested clearly in the range of strong fields ($H \sim 30$–40 kOe for temperatures 2–16 K) both upon an increase and upon a decrease in the external field (see Fig. 3). With increasing temperature, the secondary peak is shifted to the range of lower fields and becomes narrower.

After the attainment of high temperatures, the secondary peak is clearly manifested, which is demonstrated in Fig. 4 by the curve recorded at $T = 21$ K. At $T \geq 25$ K, no secondary peak could be distinguished on the $M(H)$ curves. It can also be clearly seen from Fig. 4 that in the range of strong fields, the field dependence of magnetization $M(H)$ becomes linear ($M = -\chi_1 H$), which is typical of diamagnets. Diamagnetic susceptibility χ_1 is almost the same for temperatures below T_c and is equal to 7.5×10^{-5} cm³/mol, which is close to the values of χ_1 for $Ba_{0.6}K_{0.4}BiO_3$ at 30–40 K determined in [27].

The upper critical field H_{c2} in which the direct and reverse $M(H)$ curves coincide, as well as irreversibility field H_{irr}, can be determined from the magnetization curves. The values of H_{c2} were determined for the tem-

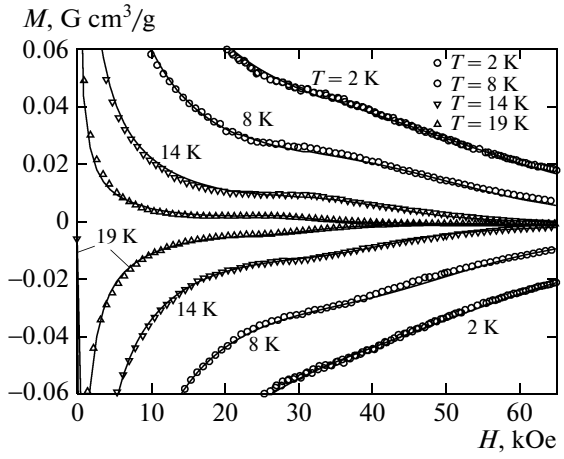

Fig. 3. Segment of magnetization loops for $Ba_{0.6}K_{0.4}BiO_3$ in the region of the secondary peak for various T. Symbols correspond to experiment; curves are calculated using ECSM with allowance for phase separation (4).

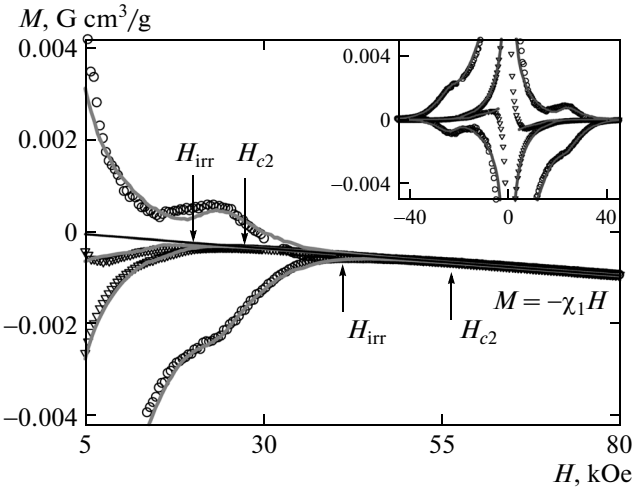

Fig. 4. Segments of magnetization loops for $Ba_{0.6}K_{0.4}BiO_3$ at $T = 21$ K (○) and 25 K (▽). Straight line is the diamagnetic contribution for $Ba_{0.6}K_{0.4}BiO_3$. Examples of determining H_{c2} and H_{irr} are illustrated. Solid curves are calculated by the ECSM with allowance for phase separation (4). The inset shows the same dependences after the subtraction of the diamagnetic contribution.

perature range above 20 K; the criterion was the beginning of coincidence of the experimental points of the $M(H)$ dependence with linear dependence $M = -\chi_1 H$. Figure 4 illustrates the determination of H_{c2} and H_{irr}.

The behavior of the $M(H)$ dependences obtained after subtraction of the diamagnetic contribution is illustrated in the inset to Fig. 4. It can be seen that the hysteretic dependences associated only with the superconductive contribution are asymmetric relative to the abscissa axis. The asymmetry of the loops decreases upon cooling.

The dependence of the pinning force in the external field was determined from magnetic measurements as $F_P(H) = J_c(H)H$, where the critical current density averaged over the sample is defined by the expression from the Bean model: $J_c = 30\Delta M/d$, where ΔM is the height of the magnetization loops in the units of G g/cm^3 and d is the sample size in centimeters. Figure 5 shows the field dependences of pinning force F_P in coordinates $f_P = F_P/F_{P1m}$ vs. $h = H/H_{irr}$ at various temperatures; here, F_{P1m} is the height of the first peak (in weak fields). The $f_P(h)$ curves) coincide in the range of weak fields and near H_{irr}, but diverge in the region of the peak effect. The values of H_{irr} were taken directly from the experimental magnetization curves $M(H)$ (see Fig. 4 as an example of determining H_{irr}); for $T = 2$ K and 8 K, these values were determined from the condition of coincidence of segments of the $f_P(h)$ curves near $H = 0$ and $H = H_{irr}$.

3. DISCUSSION

3.1. Scaling of the Field Dependences of Pinning Force

Analysis of the variation of the secondary peak height and position with temperature on the experimental $M(H)$ curves provides information on the mechanisms for the occurrence of the secondary peak. The first and secondary peaks on the $M(H)$ dependences correspond to the first and second maxima on the $F_P(H)$ curves. The secondary peak on the $F_P(H)$ curve is associated with a change in the pinning mechanism and the structure of the vortex lattice. In this case, field H_{2p} corresponding to the secondary peak coincides with the line demarcating the regions with different vortex lattices on the phase diagram of the superconductor [4]. In phase transitions, scaling in the dependences of the pinning force in coordinates $f_P =$

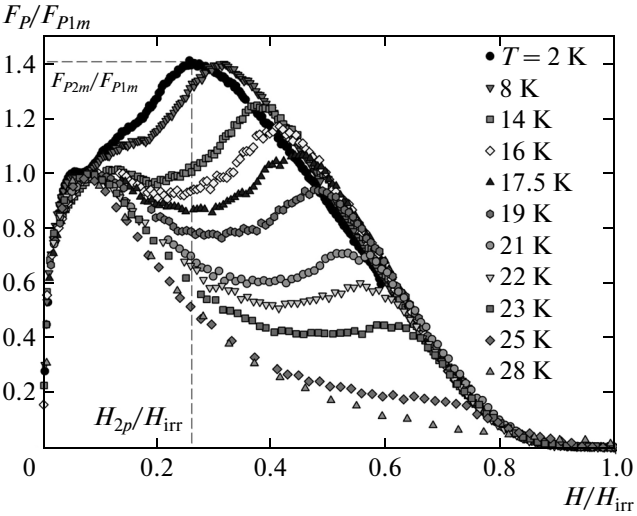

Fig. 5. Dependence of the pinning force on the magnetic field in coordinates $f_P = F_P/F_{P1m}$ vs. $h = H/H_{irr}$. The second peak on the $f_P(h)$ dependence at $T = 2$ K corresponds to the peak effect.

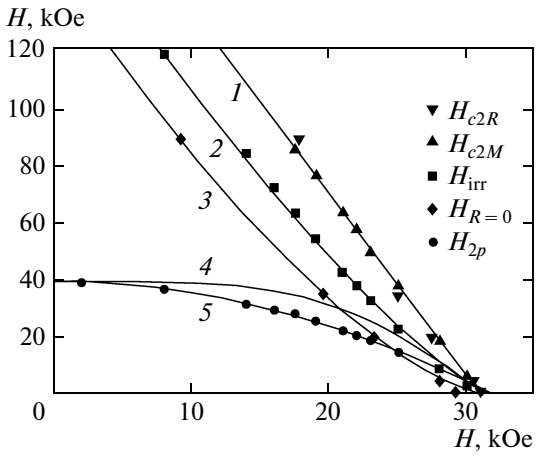

Fig. 6. Phase diagram for $Ba_{0.6}K_{0.4}BiO_3$. Symbols correspond to experimental values of the upper critical field determined from resistive ($H_{c2R}(T)$) and magnetic measurements ($H_{c2M}(T)$), as well as irreversibility fields $H_{irr}(T)$, zero-resistance fields $H_{R=0}(T)$, and fields corresponding to the secondary peak $H_{2p}(T)$. Curve *1* corresponds to $H = 198.5(1 - T/T_c)$; *2*—$H = 174(1 - T/T_c)^{1.3}$; *3*—$H = 150(1 - T/T_c)^{1.5}$; *4*—$H = 40(1 - (T/T_c)^4)^{1.4}$, and *5*—$H = 40(1 - (T/T_c)^2)$.

F_P/F_{P2m} vs. $h = H/H_{irr}$ at various temperatures must be observed in the vortex lattice [1, 28, 29], where F_{P2m} is the height of the second peak on the $F_P(H)$ curve.

For the data obtained in coordinates of $f_P = F_P/F_{P2m}$ vs. h, the dependences for different temperatures do not fit the same curve; therefore, there is no scaling in the position or in the secondary peak amplitude. It can be seen from Fig. 5 that the position of the secondary peak H_{2p}/H_{irr} changes from $h = 0.33$ at $T = 8$ K to $h = 0.6$ at $T = 23$ K, while the position of the peak in coordinates of reduced field h would remain unchanged for the expected pattern of the peak effect due to the phase transition of the lattice. It should be noted that the field corresponding to the first maximum of the pinning force in the reduced coordinates remains unchanged ($H_{1p}/H_{irr} \approx 0.09$).

3.2. Temperature Dependences of Characteristic Fields

Figure 6 shows the values of H_{2p} at different temperatures. The temperature dependence of the position of secondary peak H_{2p} makes it possible to identify the phase transition type. In phase transitions in the vortex lattice typical of layered superconductors [4], the temperature dependence of field H_{2p} has a positive curvature. Such a scenario is hardly feasible for BKBO exhibiting weak anisotropy. In the scenario of plastic pinning [3], the value of H_{2p} changes with temperature as $H_{2p} \propto (1 - (T/T_c)^4)^{1.4}$. This function coincides in the sign of the curvature with the observed dependence; however, the quantitative coincidence is poor (see Fig. 6). The observed position of the secondary peak of the pinning force is successfully described by the dependence $H_{2p} = H_{2p0}(1 - (T/T_c)^2)$ for $H_{2p0} = 40$ kOe. Such an $H_{2p}(T)$ dependence can be due to the presence of regions with a lower value of H_{c2} in the sample [30]. It is known that regions with a lower value of H_{c2} may appear when spatially separated domains differing in the chemical composition or in oxygen stoichiometry are formed in the main superconducting matrix [7]. Upon an increase in the external field, superconductivity is suppressed sooner in such regions. For an external field close to H_{2p}, the domains transformed into the normal state may play the role of effective pinning centers, which ultimately leads to the peak effect.

The suppression of superconductivity and possible growth of nonsuperconducting domains upon an increase in the external field affect the cessation of supercurrent percolation (for external field $H = H_{R=0}$) and the beginning of the flow of vortices through the sample (for $H = H_{irr}$). For $H = H_{c2}$, the entire sample passes to the normal state. Figure 6 shows the temperature dependences of H_{2p}, H_{irr}, $H_{R=0}$, and H_{2c}. In the temperature range above 18 K, the $H_{c2}(T)$ dependence is approximated by a linear function with a slope of $dH_{c2}/dT \approx -6.4$ kOe/K in accordance with the data reported in [29, 31]; at the same time, it was shown in [29] that the $H_{c2}(T)$ dependence for BKBO may have a positive curvature in a wider temperature range. The $H_{irr}(T)$ and $H_{R=0}(T)$ dependences are successfully described by functions $H = 174$ kOe $(1 - T/T_c)^{1.3}$ and $H = 150$ kOe $(1 - T/T_c)^{1.5}$, respectively. In the range $T > 25$ K, line $H_{R=0}(T)$ passes below the dependence $H = 40$ kOe $(T/T_c)^2)$. It should be noted that a clearly manifested peak effect is observed on the $M(H)$ dependences only in the temperature range below 25 K. One of the conditions for the peak effect is probably the fulfillment of the inequality $H_{R=0} > H_{2p}$ at $T = \text{const}$.

3.3. Extended Critical State Model

The asymmetry of the $M(H)$ curves relative to the axis $M = 0$, which is typical of many superconductors at high temperatures, is due to peculiarities of the pinning of vortices at the sample surface. In the extended critical state model (ECSM) [24, 32, 33] describing asymmetric magnetization loops, the degree of asymmetry is determined by the ratio of the depth L_s of the surface layer with equilibrium magnetization to characteristic sample size d (or the average grain size in the case of a polycrystal). The value of L_s is approximately equal to the magnetic field penetration depth λ_L [24, 33].

It was shown in [25] that the peak effect can be described using the ECSM. In the region of the peak effect, the value of L_s decreases as the critical current density at H_{2p} increases. The function describing the

peak of the critical current density and the corresponding suppression of L_s can be defined in the form

$$P(B) = 1 + A\exp\left(-\left(\ln\frac{|B|}{B_{2p}}\right)^2 / \left(2\frac{B_w}{B_{2p}}\right)^2\right). \quad (1)$$

Here, the peak is characterized by the position of center B_{2p}, height A relative to the initial level and width B_w. Expression (1) makes it possible to correctly define the peak in any range of the fields; in particular, the condition $P(B) = 1$ holds for $B = 0$. The field dependence of L_s with allowance for the peak effect can be written as

$$L_s(H) = \frac{L_{s0}}{\sqrt{1 - H/H_{c2}}}\frac{1}{P(\mu_0 H)}. \quad (2)$$

Here, L_{s0} is the value of L_s for $H = 0$. The first factor in expression (2) coincides with the expression for the field dependence of the Londons penetration depth [34]. The field dependence of the local critical current density, describing the peak effect, is given by

$$j_c(B) = \frac{j_{c0}}{|B|/B_0 + \exp(|B|/B_1)}P(B). \quad (3)$$

Here, j_{c0} is the value of j_c for $B = 0$; the first factor in the product is the monotonic dependence determining the behavior of $j_c(B)$ on various scales of the magnetic field [35]. In weak fields, this function behaves analogously to the dependence in the Kim model [36], while in strong fields, an exponential decrease is manifested. Coefficients B_0 and B_1 determine the rate of variation of the current densities on these scales.

The extended critical state model [24, 25] provides a correct description of the experimental magnetization loops for BKBO, which makes it possible to carry out their parameterization and to estimate the field of complete penetration (see table). Height A of the peak relative to the "unperturbed" field dependence of the magnetization exhibited a weak temperature dependence. Parameter A was o 0.5 for temperatures below 20 K; i.e., the critical current density in field $H_{2p}(T) = B_{2p}(T)/\mu_0$ was approximately 1.5 times higher than the "unperturbed" value. For high temperatures, the value of A is of the same order of magnitude, but the error in the estimated value of this parameter is larger due to the small magnetization values.

Analysis of the asymmetry of the magnetization loops makes it possible to estimate the size of the regions of screening supercurrent circulation in the sample. Using the available value of $\lambda_L = 300$ nm for BKBO [8], we obtain a size of $d \sim 20$ μm of superconducting regions at $T = 2$ K. This value is much smaller than the size of the single crystal under investigation (10^{-3} m).

3.4. Phase Separation

The peak effect due to enhancement of pinning considered in Section 3.3 is not associated with phase separation. However, phase separation into the insulating and superconducting regions is observed in BKBO in the range of fields and temperatures overlapping with the peak effect [12, 13, 37, 38]. The pattern of phase separation depends on extrinsic parameters (temperature, transport current, and magnetic field). The sizes of superconducting and insulating regions change upon partial suppression of superconductivity, which must be reflected in the $M(H)$ dependences.

Parameterization of magnetization loops. Full penetration field H_p, field corresponding to the secondary field on the $M(H)$ dependence, width B_w of the peak, and asymmetry parameter $2L_{s0}/d$

T, K	H_p, kOe	B_{2p}, kG	B_w, kG	$2L_{s0}/d$
2	1.9	40	13	0.03
8	1.6	39	9	0.045
14	1	35	6	0.06
19	0.6	26	2.5	0.1
25	0.2	15	1	0.24

To take into account phase separation in the ECSM, we introduce the magnetic-field-dependent quantity x_I determining the fraction of the insulator phase in the sample. In the case of phase separation, the sample can be visualized as an insulator matrix containing superconducting "droplets." In this case, the volume occupied by the superconducting droplets is $(1 - x_I)V$ and their average size is $d = (1 - x_I)V^{1/3}/N$, where V is the sample volume and N is the number of superconducting droplets. The magnetic field penetrates into the insulator matrix freely and only partially penetrates into the droplets, which is described by the ECSM. If the value of x_I decreases with increasing field, the value of d increases and, accordingly, the total diamagnetic response of the sample becomes stronger. The peak on the magnetization loops is observed if x_I sharply decreases with increasing field. The determination of the field and temperature dependences of x_I during phase separation requires further theoretical and experimental investigations. In this study, we chose the functional dependence $x_I(H)$ from the condition of the best description of experimental magnetization loops. We derived the following phenomenological expression:

$$x_I(H) = (x_{\max} - x_{\min}) \times \left[1 + \exp\left(\frac{\ln(|H|/H_{2p})}{H_w/H_{2p}}\right)\right]^{-1} + x_{\min}, \quad (4)$$

where $x_{\max}$ and $x_{\min}$ are the maximal and minimal fractions of the insulator phase for a preset temperature and parameter H_w determines the width of transition of x_I from $x_{\max}$ to $x_{\min}$. Solid curves in Figs. 3 and 4 show the result of description of experimental magnetization loops using the ECSM and taking into account phase separation. Figure 7 shows the variation

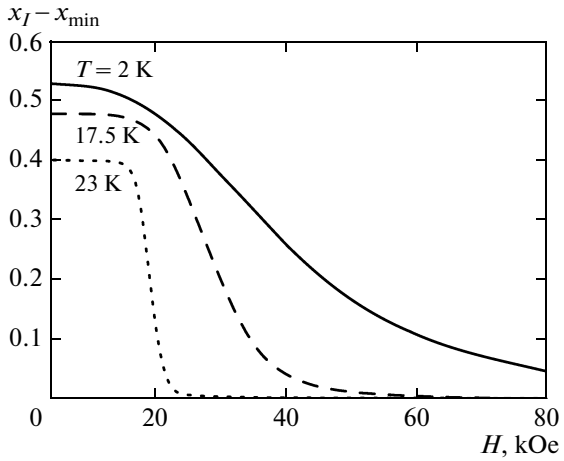

Fig. 7. Variation of the fraction of the insulator phase in $Ba_{0.6}K_{0.4}BiO_3$, obtained from the description of magnetization loops in ECSM with allowance for phase separation (4).

of x_I relative to x_{min} with the field, which was obtained in describing the magnetization loops at various temperatures. The fraction of the insulator phase was not smaller than 54% at $T = 2$ K and $H = 0$. The observed variation of magnetization in the peak effect corresponds to an increase in the fraction of the superconducting phase by 1.85 times.

With allowance for phase separation, the peak effect is reproduced for $A = 0$ in expression (1) and $P(B) = 1$ in expressions (2) and (3). Consequently, an increase in the size of superconducting regions may lead to the second peak on the $f_P(h)$ curves (see Fig. 5) even in the absence of a peak on the $j_c(B)$ dependence.

Thus, the experimental magnetization loops were successfully described by the ECSM with allowance for the variation of the size of the insulating and superconducting regions upon a change in the field and temperature. The average size $d = (1 - x_{max})D \sim 20$ μm of the superconducting regions in a weak field at $T = 2$ K (estimated in Section 3.3) is in conformity with the results of magnetooptical studies of phase separation in BKBO [37].

4. CONCLUDING REMARKS

In this study, we have investigated the field dependences $M(H)$ of the magnetization of $Ba_{0.6}K_{0.4}BiO_3$ single crystals, which demonstrate the peak effect. Our analysis of the $M(H)$, $H_{2p}(T)$, and $F_P(H)$ dependences indicates that the peak effect in $Ba_{0.6}K_{0.4}BiO_3$ is associated with phase separation [20, 23]. Hysteretic $M(H)$ dependences together with the secondary peak are described using the expanded critical state model [24, 25]. Good agreement is attained in the description of the magnetization loops both with allowance for the peak on the $j_c(B)$ dependence and using the field dependence of fraction x_I of the insulating phase. In all probability, the insulating regions corresponding to magnetic field values near H_{2p} decrease to sizes favorable for pinning of vortices on them. In this case, the peak effect is determined by the excess contribution to the magnetization due to an increase in the fraction of superconducting regions as well as by the peak of the $j_c(B)$ curve caused by enhancement of peaking.

It was shown recently by Kogan [39] that the magnetoelastic effect may lead to the peak effect on the reversible dependence of magnetization in fields stronger than the irreversibility field. The mechanism proposed in this study also allows the occurrence of such a peak effect on the reversible magnetization if phase separation is suppressed in fields stronger than H_{irr}.

REFERENCES

1. T. H. Johansen, M. R. Koblischka, H. Bratsberg, and P. O. Hetland, Phys. Rev. B: Condens. Matter **56**, 11273 (1997).
2. G. P. Mikitik and E. H. Brandt, Phys. Rev. B: Condens. Matter **64**, 184514 (2001).
3. Y. Abulafia, A. Shaulov, Y. Wolfus, R. Prozorov, L. Burlachkov, Y. Yeshurun, D. Majer, E. Zeldov, H. Wühl, V. B. Geshkenbein, and V. M. Vinokur, Phys. Rev. Lett. **77**, 1596 (1996).
4. B. Rosenstein, B. Ya. Shapiro, I. Shapiro, Y. Bruckental, A. Shaulov, and Y. Yeshurun, Phys. Rev. B: Condens. Matter **72**, 144512 (2005).
5. M. Nakamura, Y. Yamada, T. Hirayama, Y. Ikuhara, Y. Shiohara, and S. Tanaka, Physica C (Amsterdam) **259**, 295 (1996).
6. Y. Tanabe, T. Adachi, K. Omori, H. Sato, T. Noji, and Y. Koike, J. Phys. Soc. Jpn. **76**, 113706 (2007).
7. D. V. Peryshkov, E. A. Goodilin, I. A. Presnyakov, K. V. Didenko, Y. D. Tretyakov, A. Birkner, and W. Grünert, Mendeleev Commun. **14**, 161 (2004).
8. S. N. Barilo, S. V. Shiryaev, V. I. Gatalskaya, J. W. Lynn, M. Baran, H. Szymczak, R. Szymczak, and D. Dew-Hughes, Phys. Rev. B: Condens. Matter **58**, 12355 (1998).
9. A. I. Golovashkin, A. V. Gudenko, L. N. Zherikhina, M. L. Norton, and A. M. Tskhovrebov, Sov. Phys. JETP **79** (1), 163 (1990).
10. T. Klein, W. Harneit, L. Baril, and C. Escribe-Filippini, J. Low Temp. Phys. **105**, 1067 (1996).
11. T. Klein, L. Baril, C. Escribe-Filippini, J. Marcus, and A. G. M. Jansen, Phys. Rev. B: Condens. Matter **53**, 9337 (1996).
12. N. V. Anshukova, V. B. Ginodman, A. I. Golovashkin, L. N. Zherikhina, L. I. Ivanova, A. P. Rusakov, and A. M. Tskhovrebov, Sov. Phys. JETP **70** (5), 923 (1990).
13. A. I. Golovashkin, L. N. Zherikhina, G. V. Kuleshova, A. M. Tskhovrebov, and M. L. Norton, J. Exp. Theor. Phys. **102** (4), 603 (2006).
14. D. C. Kim, J. S. Kim, S. J. Joo, G. T. Kim, C. Bougerol-Chaillout, S. M. Kazakov, J. S. Pshirkov, E. V. Antipov, and Y. W. Park, J. Low Temp. Phys. **117**, 1205 (1999).

15. D. C. Kim, A. N. Baranov, J. S. Kim, H. R. Kang, B. J. Kim, Y. C. Kim, J. S. Pshirkov, E. V. Antipov, and Y. W. Park, Physica C (Amsterdam) **364–365**, 278 (2001).
16. D. C. Kim, J. S. Kim, H. R. Kang, G. T. Kim, A. N. Baranov, Y. W. Park, J. S. Pshirkov, and E. V. Antipov, Phys. Rev. B: Condens. Matter **64**, 064502 (2001).
17. E. A. Protasov, S. V. Zaitsev-Zotov, Yu. N. Venevtsev, and V. V. Bogatko, Sov. Phys. Solid State **20** (11), 2028 (1978).
18. S. V. Zaitsev-Zotov and E. A. Protasov, Sov. Phys. Solid State **26** (5), 834 (1984).
19. D. A. Balaev, A. A. Dubrovskiy, S. I. Popkov, K. A. Shaikhutdinov, O. N. Mart'yanov, and M. I. Petrov, J. Exp. Theor. Phys. **110** (4), 584 (2010).
20. A. A. Gorbatsevich, Yu. V. Kopaev, and I. V. Tokatly, JETP Lett. **52** (2), 95 (1990).
21. J. Ahmad and H. Uwe, Phys. Rev. B: Condens. Matter **72**, 125103 (2005).
22. B. A. Baumert, J. Supercond. **8**, 175 (1995).
23. A. P. Menushenkov, K. V. Klementev, A. V. Kuznetsov, and M. Yu. Kagan, J. Exp. Theor. Phys. **93** (3), 615 (2001).
24. D. M. Gokhfeld, D. A. Balaev, M. I. Petrov, S. I. Popkov, K. A. Shaykhutdinov, and V. V. Valkov, J. Appl. Phys. **109**, 033904 (2011).
25. D. M. Gokhfeld, J. Supercond. **26**, 281 (2013).
26. L. A. Klinkova, V. I. Nikolaichik, N. V. Barkovskii, and V. K. Fedotov, Russ. J. Inorg. Chem. **50** (5), 659 (2005).
27. B. Batlogg, R. J. Cava, L. W. Rupp, Jr., A. Mujsce, J. Krajewski, J. Remeika, W. Peck, A. Cooper, and G. Espinosa, Phys. Rev. Lett. **61**, 1670 (1988).
28. D. Dew-Hughes, Philos. Mag. **30**, 293 (1974).
29. V. F. Gantmakher, L. A. Klinkova, N. V. Barkovskii, G. E. Tsydynzhapov, S. Wiegers, and A. K. Geim, Phys. Rev. B: Condens. Matter **54**, 6133 (1996).
30. H. Wen and Z. Zhao, Appl. Phys. Lett. **68**, 856 (1996).
31. J. E. Graebner, L. F. Schneemeyer, and J. K. Tomas, Phys. Rev. B: Condens. Matter **39**, 9682 (1989).
32. D. X. Chen, R. W. Cross, and A. Sanchez, Cryogenics **33**, 695 (1993).
33. E. V. Blinov, R. Laiho, E. Lahderanta, Yu. P. Stepanov, K. B. Traito, and L. S. Vlasenko, J. Exp. Theor. Phys. **79** (3), 433 (1994).
34. J. R. Clem, in *Proceedings of the 14th International Conference on Low Temperature Physics (LT 14), Otaniemi, Finland, August 14–20, 1975*, Ed. by M. Krusius and M. Vuorio (North-Holland, Amsterdam, The Netherlands, 1975), Vol. 2, p. 285.
35. V. V. Val'kov and B. P. Khrustalev, J. Exp. Theor. Phys. **80** (4), 680 (1995).
36. Y. B. Kim, C. F. Hempstead, and A. R. Strnad, Phys. Rev. **129**, 528 (1963).
37. A. I. Golovashkin, A. M. Tskhovrebov, L. N. Zherikhina, L. S. Uspenskaya, and M. Norton, J. Phys.: Conf. Ser. **150**, 042043 (2009).
38. L. N. Zherikhina, A. M. Tskhovrebov, L. A. Klinkova, D. A. Balaev, S. I. Popkov, and K. A. Shaikhutdinov, J. Phys.: Conf. Ser. **400**, 022146 (2012).
39. V. G. Kogan, Phys. Rev. B: Condens. Matter **87**, 020503(R) (2013).

Translated by N. Wadhwa